Geochemical characteristics and diagenetic fluids of dolomite reservoirs in the Huanglong Formation, Eastern Sichuan Basin, China

Wen Huaguo[1, 2*], Wen Longbin[1, 2], Chen Haoru[1, 2], Zheng Rongcai[1, 2], Dang Lurui[3] and Li Yanan[1, 2]

[1] State Key Laboratory of Oil and Gas Reservoir Geology and Exploitation, Chengdu University of Technology, Sichuan 610059, China

[2] Institute of Sedimentary Geology, Chengdu University of Technology, Sichuan 610059, China

[3] Chongqing Gas District of Southwest Oil and Gas Company of CNPC, Chongqing 400021, China

Abstract: Based on a comprehensive study of texture, diagenetic behavior and evolution of dolomite in the Huanglong Formation, trace (e.g., Fe, Mn and Sr) and rare earth element (REE) geochemistry, and isotopic characteristics (e.g., C, O and Sr), four types of diagenetic fluids are identified in the Huanglong Formation dolomite reservoirs of the Eastern Sichuan Basin, China: 1): marine-derived pore waters in the marine diagenetic environment, 2) sabkha compaction brine conserved in the early shallow-buried diagenetic environment, 3) strongly-oxidizing low-temperature meteoric water in the seepage-subsurface flow diagenetic environment, and 4) strongly reducing deeply seated mixed hot brine in the middle and deep burial diagenetic environment. The fluids developed hereditarily from one environment to another, which resulted in its respective characteristics. Fluid characteristics play an important role in the development of dolomite reservoirs: 1) dolomitization by marine-derived pore water in the quasi-syngenetic stage did not form an effective reservoir; 2) early diagenetic burial dolomitization by the sabkha compaction brine formed the basis for reservoir development; 3) meteoric water karstification in the paleo-epidiagenetic stage expanded both the distribution and the size of the reservoirs, and improved the reservoir quality; 4) deep-burial dissolution and tectonic fracturing in the reburial diagenetic stage further improved reservoir porosity and permeability.

Key words: Dolomite reservoir, geochemistry, diagenetic fluids, Huanglong Formation, Carboniferous, Sichuan Basin

1 Introduction

The diagenesis of sediments is an important part of sedimentology and basin research (Milliken, 2003). The specific focuses are the fluid flow and the action process with rock, products, fluid properties, and coupling or matching relationship between diagenetic fluids and reservoirs in both time and space. These questions are at the leading edge of research in petroleum geology currently (Milliken, 2003; Li et al, 2006; Liu, 2009). Diagenesis in a reservoir is a very complex geochemical process (Zhu et al, 2009) that is significantly influenced by fluid-flow (Lai et al, 2005). There are abundant studies that have determined the reservoir diagenetic evolution and fluid properties and then analyzed the internal relationships between fluids and reservoir

development on the basis of trace and rare earth elements, as well as carbon, oxygen, and strontium isotope geochemistry (Azmy et al, 2009; Zheng et al, 2010; 2012; Corlett and Jones, 2012; Geske et al, 2012; Slater and Smith, 2012; Zhang et al, 2012; Wang et al, 2012; Azomani et al, 2013). The Paleozoic marine carbonate formations in the Eastern Sichuan Basin are one of the most significant natural gas−bearing regions in modern China, with the dolomite reservoir of the upper Carboniferous Huanglong Formation (equivalent to the Moscovian stage) being one of the basin's most significant reservoirs. Although previous studies of the sedimentary facies, reservoir features, and diagenetic systems of the Huanglong Formation are useful (Wang et al, 1996; Hu et al, 2009; Wen et al, 2009; 2011; Zheng et al, 2003; 2008; 2010), research into the relationship between diagenetic fluids and reservoir development has been insufficient, thereby affecting reservoir prediction and exploration planning. To address this gap, in this study we employ textural analysis of carbonate rocks, geochemistry characteristics of trace elements (e.g., Fe,

Mn, and Sr), rare earth elements (REE), and stable isotopes (e.g., C, O, and Sr) to reveal comprehensively the nature of fluids during various stages of dolomite reservoir diagenesis, the mechanism of water-rock reaction, and the influence of them on reservoir development, all of these mentioned above providing a strong geological basis for selecting future gas exploration targets.

2 Geological setting

The Eastern Sichuan region covers an area of 5.5×10^4 km^2 and is bounded on the east by the Qiyue Mountain, on the west by the Huaying Mountain, to the north by the Daba Mountain, and to the south by Chongqing-Kailong. This region has several high and steep NNE-NE-trending anticline structural belts from east to west (Fig. 1(a)). The Carboniferous units in the Eastern Sichuan experienced deformation during the Caledonian. Therefore, the Huanglong Formation is the only preserved strata across much of the Eastern Sichuan region. However, the Lower Carboniferous Hezhou Formation (C_1h) partially survived in the low-lying parts of this region. During the Late Carboniferous Huanglong stage, the Eastern Sichuan region was located in the Sichuan-Hubei craton basin on the eastern Yangtze Plate. That basin was a relatively sealed estuarine basin and developed a set of evaporite-carbonate sedimentary formations. The bulk of the strata unconformably overlap the dark clay shale of neritic shelf facies in the Middle Silurian Hanjiadian Formation (S_2h). At the end of the Late Carboniferous, after transient shallow burial diagenesis, the Huanglong Formation underwent paleo-epidiagenetic karstification associated with meteoric water, owing to the impact of the tectonic uplift of the Yunnan Motion during the early Hercynian. Consequently both the top ancient weathering crust and the paleokarst system developed in situ (Zheng et al, 2003; 2010; Wen et al, 2009), and the thicknesses of the residual strata are variable (Fig. 1(b)). The Huanglong Formation can be divided into three bottom-up lithological members (Fig. 2). The first member (C_2hl_1) with a residual thickness of 0-20 m is mainly of secondary-crystalline limestone. There are minor gypsum-salt rock, gypsum-bearing dolomite, secondary calcareous karst breccias in between, and evidence of the deposition from sabkhas. The second member (C_2hl_2) with a residual thickness of 12 to 50 m consists of an interbedded assemblage of grain dolomites, crystallized dolomites and karst brecciated dolomites. This member belongs to an interbedded assemblage representing a subtidal and shoal of shelf depositional environment in a semi-restricted gulf. The third member (C_2hl_3) with a residual thickness of 0-42 m consists of an interbedded assemblage of micrite, grain-bearing micrite, and micritic grain limestone. In addition, calcareous karst breccias also occur frequently as interlayers (Zheng et al, 2010). This depositional assemblage represents the combination of a subtidal and shoal of shelf facies in an open gulf environment. The reburial diagenesis occurred when the Huanglong Formation was overlain. After several tectonic events, such as Indosinian, Yanshanian, and Himalayan, buried hill gas reservoirs formed in the favorable structural areas (Wen et al, 2011).

3 Samples and methods

Samples for systematic testing and analysis were taken from 53 well cores in 19 gas-bearing structures. For petrologic identification analysis under the microscope, all the samples were collected using a micro-drill. The thin sections were identified using a microscope, and impurities and organic matter were eliminated. The procedures mentioned above were conducted to ensure the representativeness, accuracy, and reliability of the samples. The analyses of this study include thin-section observation, scanning electron microscopy (SEM) examination, X-ray diffraction (XRD) examination, trace element analysis, rare earth element analysis, and isotope analysis of carbon, oxygen, and strontium. The analytical data are shown in Appendix 1.

Double-polished casting thin sections (0.03 mm thick) were stained by Alizarin Red-S and potassium ferricyanide to distinguish calcite from dolomite and ferran carbonate from non-ferroan carbonate.

The SEM examination was performed at the State Key Laboratory of Oil & Gas Reservoir Geology and Exploitation using a Quanta 250 FEG field emission environmental SEM.

X-ray diffraction analysis was performed at the China Petroleum Exploration and Development Institute using a Rigaku D/MAX 2500 instrument at temperatures from 15 to 25 °C and humidity levels of ≤70%RH.

The analysis of the trace elements (Fe, Mn, and Sr) were conducted at Institute of Multipurpose Utilization of Minerals, Chinese Academy of Geological Sciences, Chengdu, using a Perkin Elmer 2000DV inductively coupled plasma optical emission spectrometer (ICP-OES), and the detection limit is 0.002%. The analytical standard was Y/T05-1996 of ICP broad-spectrum method.

The analysis rare earth elements (REE) were conducted at the Southwest Institute of Nuclear Physics and Chemistry, China, using the neutron activation analysis method (INAA).

The carbon-oxygen isotope test analysis was performed at the Research Institute of Exploration and Development, Southwest Oil and Gas Field Company, China National Petroleum Corporation, using an MAT252 gas isotope mass spectrometer. The analytic standard was SY/T 6039-94.

Sr isotope testing was performed at the State Key Laboratory of Oil & Gas Reservoir Geology and Exploitation using an MAT262 solid isotope mass spectrograph, and the measured inaccuracy (2σ) of $^{87}Sr/^{86}Sr$ is less than 0.006%.

4 Analysis results and discussion

4.1 Petrography

4.1.1 Genetic types of dolomites

The Carboniferous Huanglong Formation in the Eastern Sichuan region is characterized by different dolomite textures in distinct period of diagenesis, indicating multi-period and multi-genesis dolomitization. Four dolostone types could be recognized on the basis of the texture-genesis classification scheme of dolostone (Liu, 1980), and the crystal sizes and distribution of dolomite (Amthor et al, 1993). The four dolostone types are as follows: 1) the quasi-
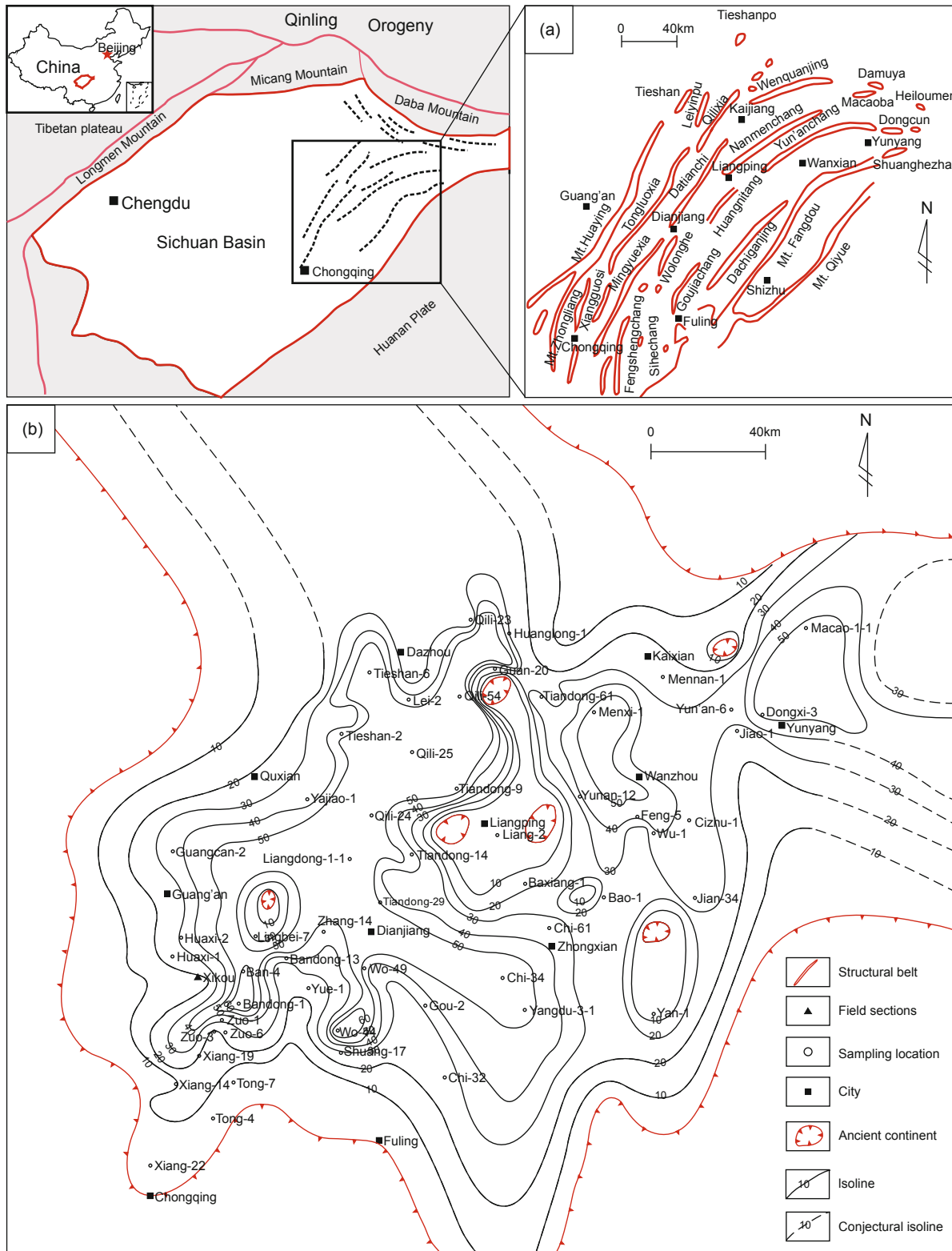
Fig. 1 (a) The tectonic map of Eastern Sichuan Basin (b) The isopach map of the Huanglong Formation

syngenetic dolomicrites (Rd1); 2) early diagenetic burial dolomites (Rd2), including residual grain dolostone and fabric-destructive powder- to finely-crystalline dolostone; 3) middle diagenetic burial dolomites (Rd3), for instance finely crystalline dolomites with dissolved pores; 4) paleo-epidiagenetic dolomites leached and transformed by meteoric

water (Bd), including grain dolomites with dissolved pores and karst brecciated dolomite. The type 1, type 2, and type 3 dolomites are of metasomatic origin, and the type 4 dolomites are formed by leaching and dissolution action associated with meteoric water. In addition, marine limestone (Ml) also occurs in the Huanglong Formation within the
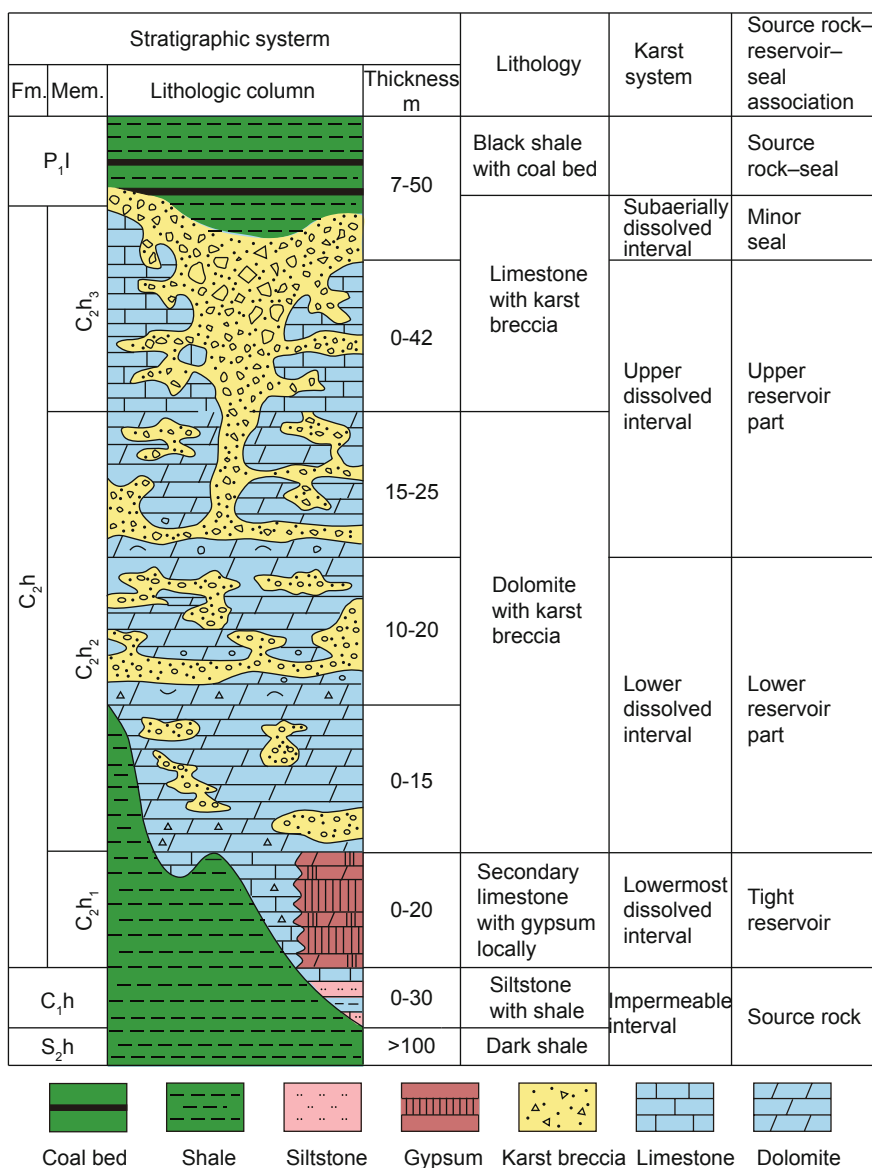
Stratigraphic systerm				Lithology	Karst system	Source rock– reservoir– seal association
Fm.	Mem.	Lithologic column	Thickness m			
P₁l			7-50	Black shale with coal bed		Source rock–seal
C₂h	C₂h₃		0-42	Limestone with karst breccia	Subaerially dissolved interval	Minor seal
					Upper dissolved interval	Upper reservoir part
			15-25			
	C₂h₂		10-20	Dolomite with karst breccia		Lower reservoir part
			0-15		Lower dissolved interval	
	C₂h₁		0-20	Secondary limestone with gypsum locally	Lowermost dissolved interval	Tight reservoir
C₁h			0-30	Siltstone with shale	Impermeable interval	Source rock
S₂h			>100	Dark shale		

Coal bed   Shale   Siltstone   Gypsum   Karst breccia   Limestone   Dolomite

Fig. 2 Integrated histogram of the paleo-karst system in the Huanglong Formation, Eastern Sichuan Basin

study area, including micrite, grain-bearing micrite (micritic grain limestone enriched with cement was eliminated), and paleo-epidiagenetic secondary limestones (Sl) leached and transformed by meteoric water, which consist of secondary-crystalline limestone and secondary brecciated limestone with a degypsumization-dedolomitization origin. The dolomite reservoirs are mainly developed in the 2nd member of the Carboniferous Huanglong Formation in the Eastern Sichuan region and are characterized by laminated and lenticular shapes. The types of reservoir rocks consist mainly of crystalline dolomites, residual grain dolostone, and karst brecciated dolomite.

1) Rd1 dolomites

The dominant lithologies are dolomicrites and gypsum-bearing dolomicrite (Fig. 3(a)) and laminar algal dolomites also can be found. The dolomite crystals are smaller than 0.01 mm in size, and have $MgCO_3/CaCO_3$ (mol·%) ratio of 0.84 (Fig. 4). Because of the high density of the dolomites, the plane porosities are always lower than 1%, and the

throat connections are poorly developed. Therefore, the Rd1 dolomites are unfavorable for reservoir development.

2) Rd2 dolomites

The Rd2 dolomites consist of residual grain dolostone (Fig. 3(b)) and powder- to finely-crystalline dolostone (Fig. 3(c)), and the dolomite crystals have subhedral to euhedral textures (Fig. 3(d)) with crystal sizes from 0.05 to 0.15 mm. The ratio of $MgCO_3/CaCO_3$ (mol·%) is 0.861 (Fig. 4). Microscopic observation of the dolomite shows recrystallization and dirty surfaces that consist of the cloudy cores and relatively clear rims (Fig. 3(c)). Intercrystalline pores and intercrystalline solution pores are well developed, and the plane porosities are always higher than 5%. Thus, the Rd2 dolomites are favorable for reservoir development.

3) Rd3 dolomites

The Rd3 dolomites are the most significant type of reservoir rocks in the Huanglong Formation, and consist of finely crystalline dolomites with dissolved pores. These dolomites are subhedral to euhedral, show obvious

recrystallization, are 0.08 to 0.25 mm in crystal size, and have a $MgCO_3/CaCO_3$ (mol·%) ratio of 0.878 (Fig. 4). Intercrystalline pores are well developed in these dolomites. A proportion of intercrystalline pores were improved by dissolution and evolved to intercrystalline solution pores which are well-connected and are filled by bitumen (Fig. 3(e)), and plane porosities range from 7% to 10%. Therefore, the Rd3 dolomites, which were continuously modified by meteoric water leaching and paleo-epidiagenetic karstification, are favorable for the development of the best reservoirs.

4) Bd dolomites

The Bd dolomites are made up of two dolomite lithologies. The first is the porous grain dolomite that originated from the leaching by meteoric water (Fig. 3(f)), and the second is karst breccias filling paleo-karst caves (Fig. 3(g)). More than 90% of the karst breccias are dolomitic (Fig. 3(h) and (i)), and the rest are calcitic (Fig. 3(j)). The Bd dolomites developed under the control of lithological factors and the paleo karst geomorphic zonation. The porous grain dolomites, which are related to reservoir development, exhibit plane porosities of 8% to 10% (with a maximum of more than 16%), and the karst brecciated dolomites (Fig. 3(j)) have the plane porosities of 5% to 8%.

4.1.2 Diagenetic environments and classifications

On the basis of the Chinese division of diagenetic stages in carbonate rocks (SY/T5478-2003), five evolutionary stages of the Huanglong dolomite reservoir in Eastern Sichuan Basin can be recognized. The five stages could be observed as a progressive succession of diagenesis, and correspond to five diagenetic environments, including: 1) the quasi-syngenetic marine diagenetic environment; 2) the early diagenetic shallow burial diagenetic environment; 3) the paleo-epidiagenetic meteoric vadose-phreatic diagenetic environment; 4) the middle- to deep-burial diagenetic environment formed during reburial; and 5) the late tectonic uplift diagenetic environment (Fig. 5).

1) Marine diagenetic environment

During the early Huanglong stage, a sabkha sedimentary environment dominated the Eastern Sichuan region near the paleo-continent that was influenced by the paleo-topography and hot-arid climate. The carbonate sediments were syngenetically dolomitized by high-salinity, evaporative pore waters during repeated episodes of evaporative pumping (Wang et al, 2001; Hu et al, 2009). This effect produced the Rd1 dolomites.

2) Shallow burial diagenetic environment

As the sediments were buried and separated from the marine environment, temperature and pressure became increasingly important. At burial depths of less than 1,000 m (shallow burial diagenetic environment), the syndepositional marine-derived pore waters in the formation were drained out, and then formed fluids associated with compaction, and always leading to pressure solution and the formation of stylolites. During the neomorphism of sediments, the regular marine limestones (Fig. 3(l)) were replaced (through metasomatism) by Mg-rich pore fluids and this shallow burial dolomitization and recrystallization resulted in the formation

of Rd2 dolomite.

3) Meteoric vadose-phreatic diagenetic environment

After the two diagenesis stages mentioned above, the Huanglong Formation was uplifted by the Yunnan Motion during the early Hercynian and evolved into a continental environment. Accordingly, the diagenetic environment also evolved into the paleo-epidiagenetic meteoric vadose-phreatic stage. The ancient weathering crust and corresponding lithologic system of paleo-karst in the same horizon have been widely developed by the influence of leaching and dissolution action associated with meteoric water (Fig. 2). The major products of this diagenetic environment are Bd dolomites and void- or fracture-filling dolomite cements. With the increase of tectonic uplift and paleo-karstification, the gypsum-salt rock and gypsum-bearing dolomite in the sabkha environment of the 1st member in the Huanglong Formation were dedolomitized and degypsified by leaching and modifying by meteoric waters. Consequently, secondary limestone (Sl) was developed with pseudomorphs of dolomite or gypsum crystals, and also with residual "cloudy cores and clear rims" structure. These kinds of secondary limestone consist of secondary crystalline limestone (Fig. 3(m)) and secondary calcareous karst breccias (Fig. 3(j)).

4) Middle-deep burial diagenetic environment

The Huanglong Formation was reburied and overlain by the Upper Permian coal measures. With an increase of burial depth, the diagenetic environment evolved from a meteoric diagenesis stage to a semi-closed deep-burial meso-diagenesis stage. The brines in the formation and the hydrothermal fluids (ascending along faults/fractures) mixed together, producing hybrid hot brines. These fluids promoted dolomitization and recrystallization (Fig. 3(e)), and produced the Rd3 dolomites. In addition, the compaction-released water from the Liangshan Formation (P_1l) coal measures and the muddy source rocks of the underlying Middle Silurian sediments mixing with the acidic hydrothermal fluids formed from decarboxylation during the maturation of organic materials re-dissolved and enlarged the existing pores, vugs, and bedrock fractures. This effect was favorable for reservoir development and is characterized by (a) dissolved and modified pores, vugs, and fractures sometimes lined by bitumen but without exotic fillings (Fig. 3(e)), and (b) the occurrence of hydrothermal indicators, such as anhedral dolomite, ankerite, quartz, celestite, fluorite, pyrite, and albite (Fig. 3(n), (o), and (p)).

5) Late tectonic uplifting diagenetic environment

During the late reburial diagenesis, the Carboniferous of the Eastern Sichuan region was influenced by the late Yanshanian-Himalayan tectonic movement and was folded, uplifted, and pervasively fragmented. The rocks were fragmented into uneven blocks by a network of straight, curved, or bifurcated fractures (Fig. 3(p)). In addition, compaction micro-fractures and re-dissolved fractures also formed in this diagenetic stage, and connected the solution pores with moniliform distribution.

As stated previously, different stages correspond to different diagenetic environments, fluids, processes, and pore evolution (Fig. 5). Burial dolomitization, paleo-karstification,
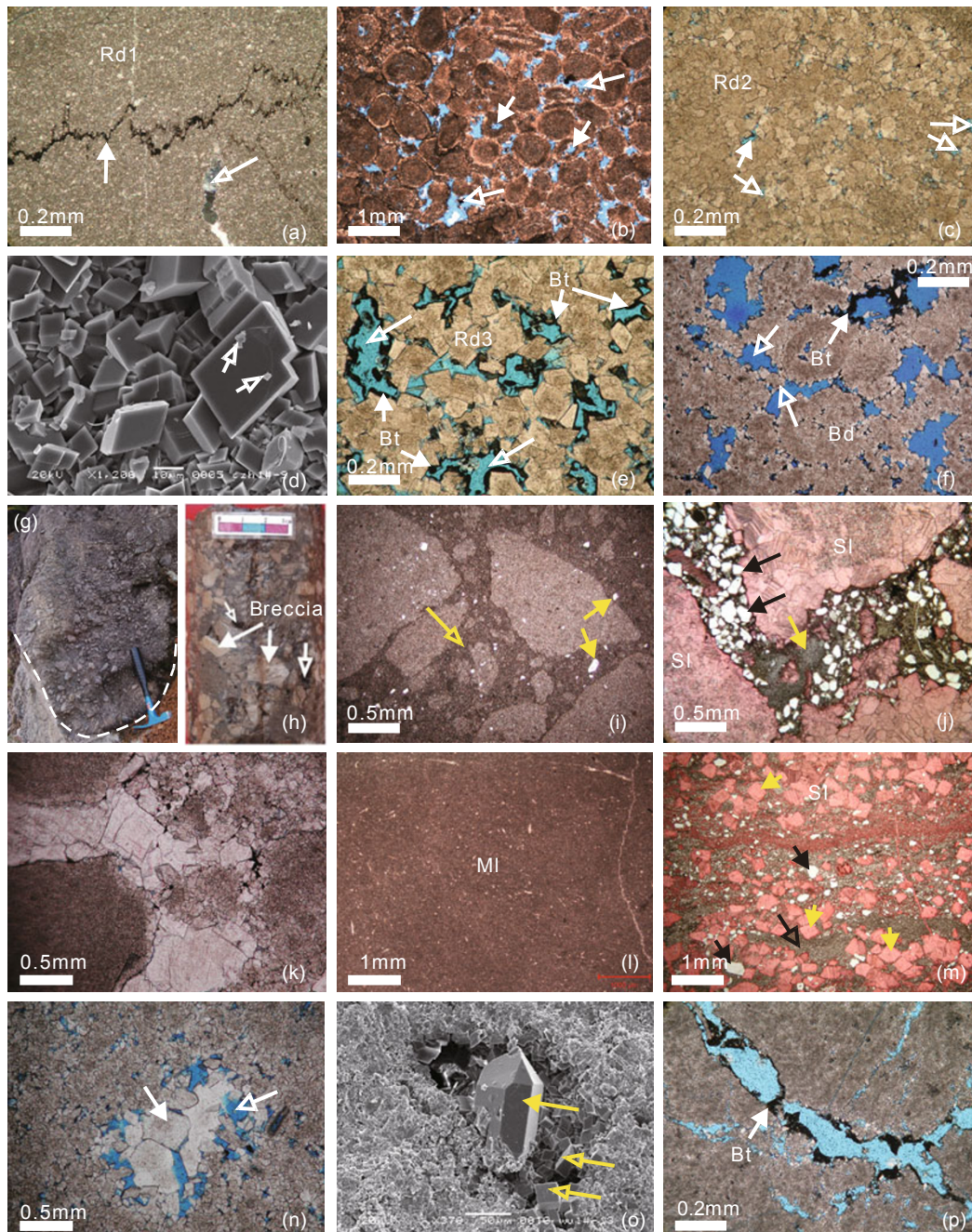
Fig. 3 Normal petrofabric and diagenesis types of carbonate in the Carboniferous Huanglong Formation of the Eastern Sichuan Basin

(a) Rd1 dolomites, gypsum-bearing dolomite with bitumen filled in the stylolites (white arrow), locally developed gypsum (hollow arrow), micrograph (+); (b) sparry oolitic dolomite with intragranular dissolved pores and intergranular dissolved pores developed in it (hollow arrow), micrograph (+); (c) Rd2 dolomite with intercrystalline dissolved pores and intercrystalline pores developed in it (hollow arrow), micrograph (+); (d) Rd2 dolomite, rhombic crystals and intercrystalline pores and illite developed in it (hollow arrow), SEM photograph; (e) Rd3 dolomite, intercrystalline dissolved pores (hollow arrow) developed and bitumen filled in it, micrograph (+); (f) sparry algal-dolarenite with intercrystalline dissolved pores (hollow arrow) developed and powder-fine crystal fresh-water dolomite and bitumen (Bt) filled in it, micrograph (+); (g) karst brecciated dolomite fill in paleo-karst caves, field photograph, the geologic hammer is 29 cm long; (h) karst brecciated dolomite with breccia-supported and a large number of dissolved pores (hollow arrow) in it, core photograph; (i) karst brecciated dolomite, the interspace in the breccia is filled by micritic dolomite matrix (hollow arrow) and quartz silt, micrograph (+); (j) karst brecciated secondary limestone, matrix in the interspace of breccias contains exotic muddy (yellow arrow) and quartz silt (black arrow), micrograph (-); (k) karst brecciated dolomite, and the breccia interspace is filled by bright and clear fresh-water macrocrystalline dolomite, micrograph (-); (l) micrite, staining thin section micrograph (-); (m) secondary crystalline limestone from dedolomitization associated with meteoric water leaching, the calcite crystals retain the crystal shapes of dolomite (yellow arrow), and the crystal interspace is filled by exotic mud (hollow arrow) brought in by groundwater and quartz silt (black arrow), indicating that the secondary limestone is the product of karstification, staining thin section micrograph (-); (n) sand-residual powder dolomite, and the intercrystalline dissolved pores (hollow arrow) are filled by hydrothermal special-shaped dolomite (solid arrow), micrograph (+); (o) powder crystalline dolomites with dissolved pores filled by secondary dolomite crystals (hollow arrow) and authigenic quartz crystals; (p) dissolved crack with bitumen remaining in its wall, micrograph (+).
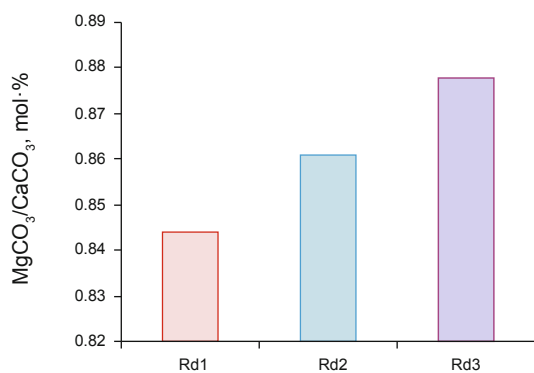
Fig. 4 Histogram of the ratios of MgCO₃/CaCO₃ (mol·%) in Rd1, Rd2, and Rd3 dolomites

deep-burial dissolution, and fragmentation are constructive diagenesis for reservoir development.

4.2 Geochemical characteristics

4.2.1 The trace element (Fe, Mn, and Sr)

Table 1 summarizes the trace element (Fe, Mn, and Sr) concentrations of 85 carbonate samples in the Huanglong Formation. According to the scatter diagrams, various types of carbonate rocks possess regular variation tendency and are described as follows (Fig. 6(a) and (b)):

1) The strontium (Sr) content of all carbonate samples ranges from 15 ppm to 340 ppm (Fig. 6(b)) with an average of 81 ppm. The overall Sr content in this study is lower than
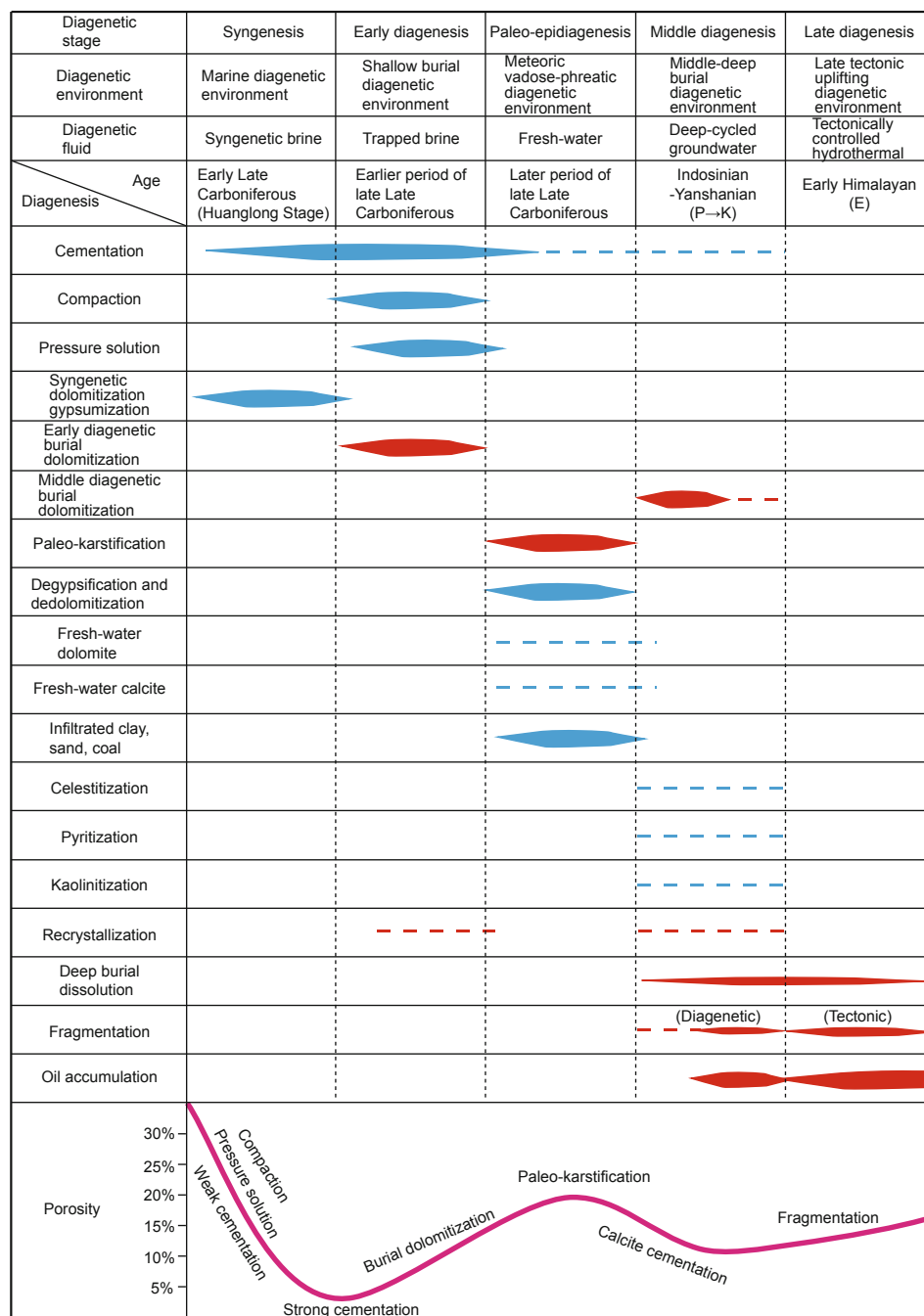

Fig. 5 The classification and evolutionary model of diagenesis in the Carboniferous Huanglong Formation, Eastern Sichuan Basin

the lower limit for standard marine samples (200 ppm) (Derry et al, 1989). The average content of Sr in Ml micrite (the most representative rock of seawater) is only 146 ppm, indicating that continental fresh waters have a large influence on the marine carbonates.

2) Theoretically, the partition coefficient of strontium in dolomite is half as high as in calcite; thus, the dolomitization of calcite or aragonite is a strontium-loss process (Huang et al, 2006; 2008). As the Ml limestones evolved from the Rd1 dolomites to the Rd2 dolomites, the Fe and Mn contents increased from 603 ppm and 67 ppm, respectively, to 1,636 ppm and 141 ppm, respectively, whereas the Sr content decreased from 146 ppm to 71 ppm. This geochemical evolution is consistent with the understanding that the burial diagenesis of carbonates is a process with Fe and Mn enrichment and strontium depletion (Veizer, 1983). The Sr content of the Rd1 dolomites (132 ppm) is less than that of the Rd2 dolomites, and this phenomenon is possibly related to the high salinity environment of Rd1 dolomites (Liu et al, 2008).

3) The Rd3 dolomites have higher average strontium content, higher average Mn content (242 ppm), and higher average Fe content (2,188 ppm) than Rd2 dolomites, suggesting that the mesodiagenetic burial Rd3 dolomites have undergone the same processes of strontium depletion that the Rd2 dolomites have experienced. Rd3 dolomitization, however, included extensive fluid concentration and strontium enrichment and, consequently, could be considered to have occurred in a relatively closed system. The Mn-enrichment and Fe-enrichment indicate that the Rd3 dolomites were also influenced by strongly reduced hydrothermal fluids (Huang et al, 2006; Zhang et al, 2008). In addition, the burial reducing environment contributes Fe and Mn from fluids to enter the dolomite crystal lattice during the diagenesis process (Zhu et al, 2012), and higher Mn content may also be associated with the hydrothermal effects (Zhang et al, 2008).

Karstification is the most significant geological process that involves meteoric waters in the alteration of the carbonates. At the end of the Huanglong stage, exposure and karstification led to the enrichment of Fe and Mn in carbonate strata near the unconformity (Fig. 6(a)). The Bd secondary limestones have higher Fe content (3,754 ppm), higher Mn content (except the Sl) (195 ppm) and lower Sr content (35 ppm) than Ml micrite, Rd1 and Rd2 dolomites, indicating that they developed under full-open karstification with meteoric water (Huang et al, 2006; 2008). Three reasons for this are as follows: (a) meteoric waters have higher Mn and lower Sr contents than depositional fluids (marine) (Walter et al, 2000; Huang et al, 2008); (b) Fe and Mn, with high valence in oxidizing conditions, cannot significantly enter dolomite crystal lattice, but they can fill in the matrix of breccias by meteoric water leaching, explaining the increase in the rocks; (c) Sr contained in fluid is drained away because Ca in dolomite is hard to replace (Huang et al, 2008).

Table 1 Sr, Mn, Fe, ΣREE, δCe, δ^{13}C, δEu, δ^{18}O and ^{87}Sr/^{86}Sr statistics for the Huanglong Formation carbonates

Types		Sr, ppm	Mn, ppm	Fe, ppm	ΣREE, ppm	LREE/HREE	δCe	δEu	$\delta^{13}C_{VPDB}$, ‰	$\delta^{18}O_{VPDB}$, ‰	^{87}Sr/^{86}Sr
Ml	No. of samples	7	7	7	5	5	5	5	6	6	6
	Average	146	67	603	56.87	28.06	0.64	0.96	-1.145	-7.206	0.7094
	Maximum	190	81	780	60.66	33.19	0.73	1.05	-0.651	-3.301	0.7138
	Minimum	90	52	420	53.32	25.79	0.54	0.87	-1.73	-9.32	0.7070
Rd1	No. of samples	14	14	14	9	9	9	9	11	11	11
	Average	132	113	952	11.62	27.8	0.78	1.07	2.813	-1.77	0.7128
	Maximum	374	155	1600	17.46	35.38	0.91	1.20	3.95	-1.14	0.7180
	Minimum	66	66	760	3.32	21.94	0.63	0.93	1.774	-3.04	0.7095
Rd2	No. of samples	35	35	35	9	9	9	9	28	28	28
	Average	71	141	1636	23.27	18.58	0.77	1.23	1.960	-3.196	0.7134
	Maximum	270	300	2900	56.22	39.77	0.99	1.46	3.84	-2.039	0.7204
	Minimum	18	52	450	1.68	5.00	0.46	1.00	0.2	-5.67	0.7075
Rd3	No. of samples	13	13	13	7	7	7	7	13	13	13
	Average	76	242	2188	6.68	20.44	0.72	1.71	1.468	-5.258	0.7128
	Maximum	130	460	3200	11.47	36.23	0.86	2.68	3.339	-3.125	0.7149
	Minimum	28	170	1100	3.11	11.97	0.61	1.25	0.36	-8.891	0.7092
Bd	No. of samples	16	16	16	6	6	6	6	16	16	16
	Average	35	195	3754	5.02	15.44	0.79	0.89	1.921	-4.033	0.7150
	Maximum	71	320	6100	5.90	20.05	0.87	0.93	3.942	-2.44	0.7200
	Minimum	15	120	820	4.21	11.51	0.64	0.85	0.33	-5.525	0.7065
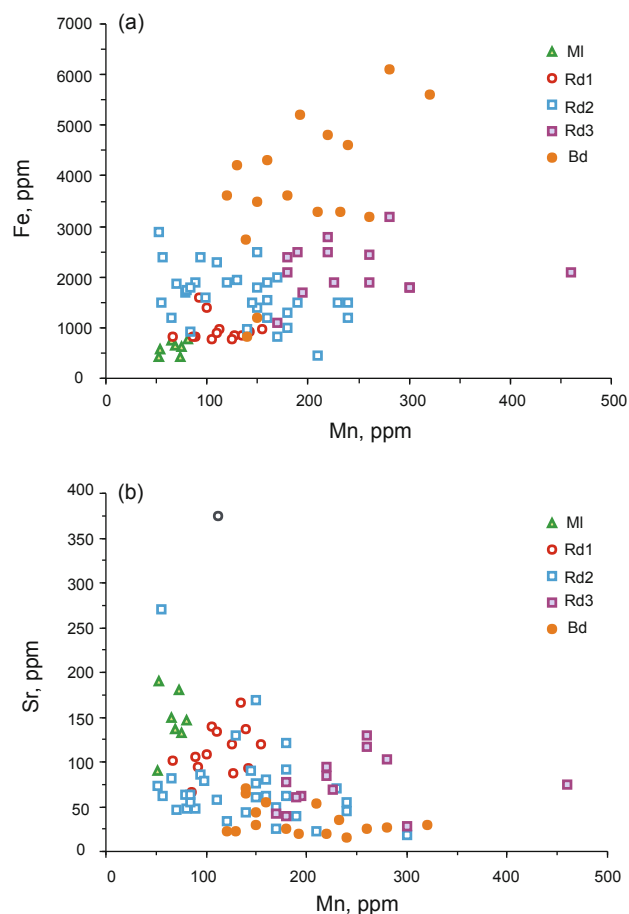
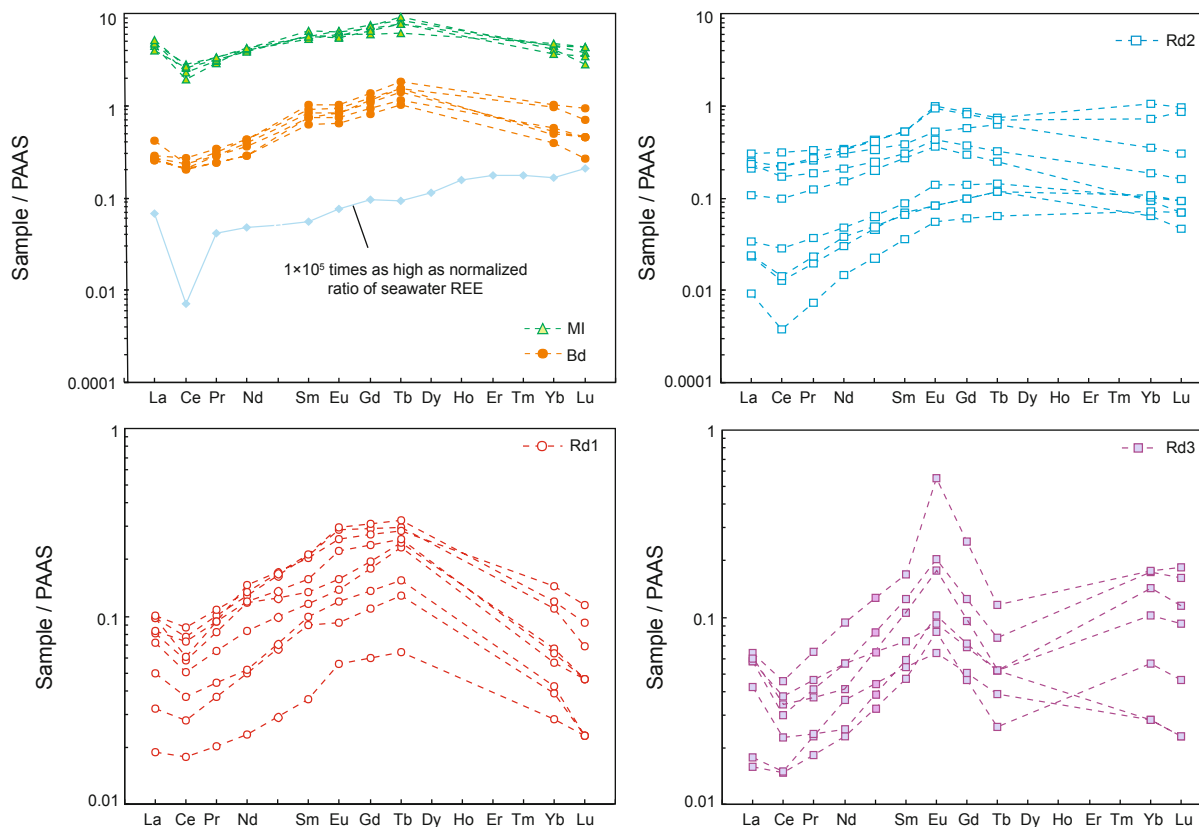**Fig. 6** Scatter diagrams of (a) Mn vs Fe and (b) Mn vs Sr for all carbonate phases in the Huanglong Formation

4.2.2 Rare earth element (REE)

According to REE analytic data of 34 samples (Table 1), the REE characteristics in different diagenetic stages are as follows:

1) The REE Post-Archean Australian Sedimentary rocks (PAAS) standardized distribution patterns (Fig. 7) show light REE enrichment and similar REE patterns for each sample, reflecting the selection and classification of them are reliable. In addition, the Ml marine micrite possesses a significantly negative Ce anomaly (0.54-0.73), and its REE distribution curve is similar to that of seawater (Han et al, 2009), indicating that the Ml marine micrite reflects the features of seawater well. The marine limestone (Ml) samples have the highest ΣREE (56.87 ppm), whereas the ΣREE for other samples is low (Table 1, Appendix 1). These values of ΣREE show that the fluids vary according to the migration and depletion of REE, and this phenomenon attributes to the redistribution and rebalance of REE between diagenetic fluids and original rocks.

2) The degree of negative Ce anomaly can reflect the degree of oxidation in the water body (Frimmel, 2009). The δCe mean value for Rd1 dolomite (0.78) is much higher than that in the Ml micrite (0.64) reflecting that the diagenetic fluid is more oxidizing depending on the increasing temperature, and this feature proves that the diagenetic fluids originated as concentrated brine from evaporation in a sabkha environment (Hu et al, 2009). The δCe mean values of Rd2 and Rd3 dolomites (0.77 and 0.72 respectively) present a gradually decreasing trend compared to that of Rd1 dolomite, reflecting that the diagenetic environment evolves into a burial environment which has stronger sealing properties and is

Fig. 7 The REE PAAS standardized distribution patterns of all types of carbonate samples in the Huanglong Formation

more reducing. The negative Ce anomaly of Bd dolomite is remarkably weakened compared with that of Rd1, Rd2, and Rd3 dolomites, indicating that the formation of this type of rock is under the open and oxidizing conditions. This induces Ce^{4+} to enter the crystal lattice of reprecipitated carbonate minerals (Han et al, 2009), and thus lead to the high δCe.

3) A positive Eu anomaly is often considered to be related to hydrothermal fluid impact and a reducing environment (Götze et al, 2001; Wang et al, 2009). The negative Eu anomaly (0.96 on average) of Rd1, Rd2, and Rd3 dolomites presents a gradually decreasing trend compared to that of Rd1 dolomite, reflecting diagenesis occurred in a relatively closed reducing burial environment of gradually increasing temperature. Rd3 dolomite has the highest positive Eu anomaly (1.71 on average), and this provides sufficient geochemical evidence to suggest that the diagenetic fluid of this type of rock is hydrothermal fluid in a middle-deep burial reducing environment. Bd dolomite presents a more remarkable negative Eu anomaly than Rd2 and Rd3 dolomites which are in the burial environment, this clearly show that diagenesis occurred in an open and oxidizing diagenetic system, and the diagenetic fluids not only have low temperatures and strong oxidizing ability but also have a strong dilution effect on Eu.

4.2.3 Oxygen and carbon isotopes

Oxygen and carbon isotope ratios of 74 samples from the Huanglong Formation were measured in all dolomites (Rd1, Rd2, Bd, and Rd3) and in micrite Ml (Table 1; Fig. 8). The mean values of $\delta^{13}C$ and $\delta^{18}O$ in the Huanglong Ml micrite are −1.145‰ (VPDB) and −7.206‰ (VPDB), respectively. The mean $\delta^{13}C$ (VPDB) values of Rd1, Rd2, and Rd3 dolomites (2.813‰, 1.960‰, and 1.468‰, respectively) are more depleted in the heavy carbon isotope, and their mean $\delta^{18}O$ values decrease from –2.96‰ (VPDB) in Rd1 to –4.749‰ (VPDB) in Rd3. The Bd dolomite has average $\delta^{13}C$ (VPDB) value of 1.921‰ and average $\delta^{18}O$ (VPDB) value of −4.033‰.

The abundance of ^{13}C and ^{18}O in marine carbonate is controlled by sea-level fluctuation, the source and embedding velocity of organic carbon, and the oxidation-reduction conditions of sedimentary-diagenetic environment (Zheng and Chen, 2000). The carbon and oxygen isotopes of original carbonate rocks would change due to the chemical precipitation, dissolution, recrystallization, and metasomatism of carbonate cements. Although the oxygen and carbon isotope data in the different types of dolomites in the Huanglong Formation of the study area have some overlap (possible related to the inherited development and evolution of Rd1, Rd2, Rd3, Bd dolomites), in dot plots they show a distinct zonation (Fig. 8). These fully reflect that the differences in sedimentary-diagenetic environments and diagenetic fluids would lead to correspondingly different carbon and oxygen isotope compositions in carbonates. There are five distinctive features of carbon and oxygen isotopes in the Huanglong Formation.

1) The lower $\delta^{13}C$ and $\delta^{18}O$ values (Table 1; Fig. 8) of the different carbonates in the Huanglong Formation relative to those carbonates formed from Moscovian original seawater suggest a possible influence of $\delta^{13}C$- and $\delta^{18}O$-depleted fluids
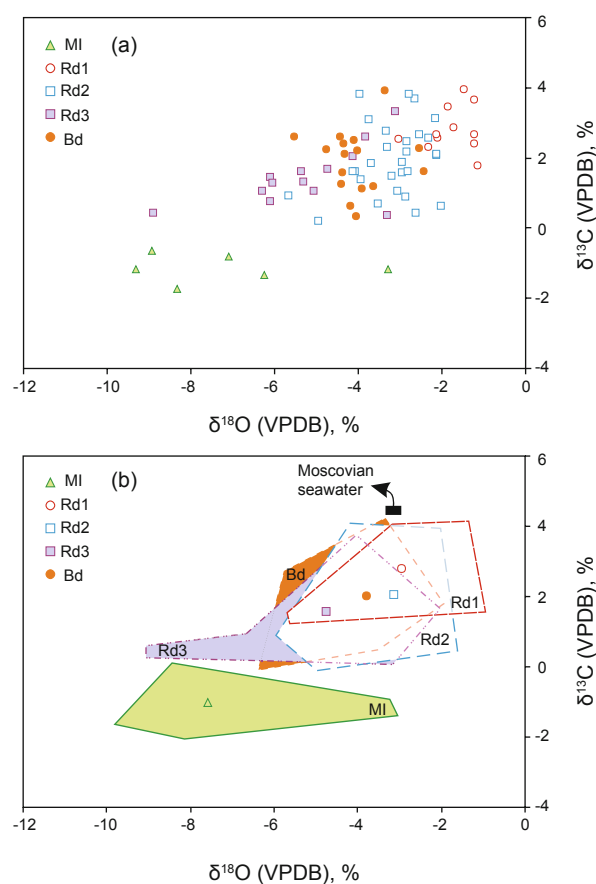

Fig. 8 (a) Cross-plot of individual oxygen and carbon stable isotope ratios of various carbonate phases in the Huanglong Formation. Data are listed in Appendix 1. (b) Fields for the various carbonate phases in this study with an average for each type of carbonate. The black square represents the range of isotopic composition of carbonates precipitated from the late Carboniferous (Moscovian) seawater (Veizer et al, 1999).

in the diagenetic system. This geochemical anomaly might be related to extensive meteoric-water leaching in the Huanglong carbonates during paleo-epidiagenesis.

2) In comparison with the micrite (Ml), the quasi-syngenetic Rd1 dolomites exhibit a positive deflection in $\delta^{13}C$ mean values of 3.958‰ (Table 2). The positive carbon isotopes reflect a marine basin that was relatively closed and strongly evaporative during the depositional period. At the same time, ^{12}C-rich CO_2 preferentially escaped from the surface of sea water (Liu et al, 2001), causing ^{13}C enrichment in seawater and consequently ^{13}C enrichment in syngenetic dolomites of the seawater. Using the isotopic data to calculate salinity index (Keith and Weber, 1964) yields a mean Z value of 132.2. This high Z value reflects diagenetic fluids that have features of high salinity brines.

3) The $\delta^{18}O$ and $\delta^{13}C$ values of Rd2 and Rd1 dolomites partially overlap (Fig. 8), suggesting that the fluids forming Rd2 dolomite might have originated from the strata-trapped brines of the earlier sabkha environment. However, the Rd2 dolomites have slightly negative $\delta^{18}O$ and $\delta^{13}C$ values compared to the Rd1 dolomites (Table 1), reflecting a decrease in dolomite-fluid isotope fractionation during an increase in both temperature and pressure in the relatively

closed, shallow-burial diagenetic environment and, finally, leading to an isotope decline in Rd2 dolomites (Huang et al, 2007).

4) Compared with Rd1 and Rd2 dolomites, the Bd dolomites have a negative deflection in $\delta^{18}O$ and $\delta^{13}C$ values. The negative isotopic shift is connected with extensive meteoric-water leaching in an open diagenetic environment during early Hercynian tectonic uplift (Gasparrini et al, 2006), and it should be noted that the atmosphere-derived CO_3^{2-} in meteoric-water have ^{12}C and ^{16}O enrichment (Veizer et al, 1999; Azmy et al, 2009). As the dissolution of meteoric water became more and more intensive, it has a stronger influence on the isotopic compositions of carbonates (Smith, 2006), and make $\delta^{18}O$ values of Bd dolomites show a clear negative depletion characteristic.

5) Rd3 dolomites have lower $\delta^{18}O$ and $\delta^{13}C$ values than Rd1, Rd2, and Bd dolomites due to the evolution of the diagenetic environment from paleo-epidiagenesis with open meteoric waters to semi-closed and deep-burial mesodiagenesis. The interpretations include the extensional tectonic settings of the late Hercynian Dongwu deformation, the influence of deep-seated ^{18}O-depleted hydrothermal fluids (Lavoie and Chi, 2006), and ^{13}C-depletion due to introduction of organic carbon from released water during the maturation of organic materials (Azmy et al, 2009).

4.2.4 Strontium isotopes

Strontium isotopic data from 74 samples (Table 1; Fig. 9) shows four primary characteristics.

1) The average $^{87}Sr/^{86}Sr$ ratio of marine limestone (Ml) is 0.7094 (Table 1) and is higher than the range of $^{87}Sr/^{86}Sr$ ratio for Moscovian (Late Carboniferous) marine limestones (Veizer et al, 1999). This isotopic anomaly could be attributed to the sedimentary environment of the Huanglong Formation in the Eastern Sichuan region. At that time, the study area was a semi-closed gulf that was restricted and surrounded by a large paleo-continent. Significant quantities of crust-derived strontium (enriched in ^{87}Sr) were carried from the paleo-continent to the basin, thereby leading to a significant increase in the basin $^{87}Sr/^{86}Sr$ ratio.

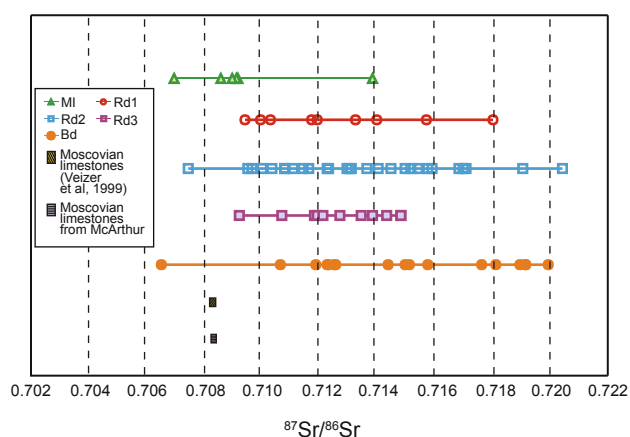2) The Rd2 dolomite that was formed in the burial diagenetic environment has a slightly higher average $^{87}Sr/^{86}Sr$ ratio (0.7134) than that of Rd1 dolomite, suggesting that the ^{86}Sr content in dolomite decreases with the deepening of the dolomitization process, thereby leading to an increase of ^{87}Sr content (Huang et al, 2006) and also the corresponding $^{87}Sr/^{86}Sr$ ratio. The average $^{87}Sr/^{86}Sr$ ratio of the Rd3 dolomite (0.7128) is almost the same as that of Rd1 dolomite, suggesting that the burial dolomitization fluids originated in the sabkha brines that were trapped in the formation (Li et al, 2006).

3) If we set the average $^{87}Sr/^{86}Sr$ ratio of marine limestones as the reference, we would find that the $^{87}Sr/^{86}Sr$ ratios of different carbonates have a gradual and simultaneous increase with the increase of the intensities of diagenesis or dissolution during diagenetic and paleo-epidiagenetic stages (Fig. 9). These characters indicate that different diagenetic fluids were influenced by surface water with crust-derived strontium enrichment, and the corresponding enrichment effect for highly radioactive ^{87}Sr existed.

4) The Bd dolomites that were modified by meteoric-water leaching have a higher average $^{87}Sr/^{86}Sr$ ratio (0.7150) than Ml micrite, or Rd1, Rd2 and Rd3 dolomites. This could be interpreted to be due to the infusion of highly radioactive ^{87}Sr during the dissolution of host dolomites and recrystallization of dolomite with ^{87}Sr-rich meteoric waters.

4.3 Diagenetic fluid and reservoir development

As mentioned above, by combining different controlling factors of reservoir development with an analysis of geochemical characteristics, the dolomite reservoir diagenetic fluids in the Huanglong Formation of Eastern Sichuan can be divided into four types, which have a diverse nature and are well connected with reservoir development.

1) After evaporation and concentration, marine-derived pore water in the marine diagenetic environment was characterized by high Sr content, positive Eu anomaly, slightly positive $\delta^{13}C$ and $\delta^{18}O$, and a high $^{87}Sr/^{86}Sr$ ratio. These characteristics resulted in the formation of dolomicrites during penecontemporaneous dolomitization, which were dominated by compaction, pressure solution, and cementation that blocked the primary pores and consequently hindered reservoir development.

2) Conserved in the early sabkha, the burial formation brine in the shallow burial diagenetic environment had low Sr content, positive Eu anomaly, slightly negative $\delta^{13}C$ and $\delta^{18}O$, and high $^{87}Sr/^{86}Sr$ ratios. As the burial depth increased, the fluid gradually became hotter and more reducing. The extensive burial dolomitization and recrystallization with the compaction brine produced the Rd2 dolomites and favored the development of intercrystalline pores. Therefore, this reservoir is better developed.

3) The strongly oxidizing low-temperature meteoric water in the seepage-subsurface flow diagenetic environment was characterized by Fe and Mn enrichment, weakly negative Ce anomaly, negative $\delta^{13}C$ and $\delta^{18}O$, and an extremely high $^{87}Sr/^{86}Sr$ ratio. Its primary process was the strong dissolution by meteoric water, yielding a characteristic karst reservoir

Fig. 9 $^{87}Sr/^{86}Sr$ ratios of the various carbonate phases in the Huanglong Formation compared to those of Moscovian limestones. Data are listed in Appendix 1

(Loucks, 2004; Breesch et al, 2009). The Bd dolomites that experienced meteoric-water leaching and modification had abundant well-developed intergranular pores and intercrystalline pores, as well as notably large intercrystalline solution pores and fractures, and was consequently the most suitable rock type for reservoir development.

4) The strongly reducing and deeply seated mixed hot brine in the medium-deep burial diagenetic stage was characterized by Mn and Fe enrichment, slightly positive Eu anomaly, and negative $\delta^{13}C$ and $\delta^{18}O$. This hot fluid formed in an extensional setting during the Hercynian Dongwu Movement when the formation water from the Carboniferous flowed through the fracture system and mixed with deep-seated hydrothermal fluids. Although early diagenesis was destructive to the dolomite reservoir (e.g., yielding cementation and partial dissolution, filling), NE-trending deep fractures and secondary faults (Zhao, 2005) formed in the study area during the late Indo-Chinese epoch-Yanshanian. These fractures are linked to the acidic decarboxylation hydrothermal fluid (which was formed after the organic matter experienced thermal evolution) that expanded the reservoir storage space. Therefore, the fractures played a crucial role in the formation of effective storage space in the dolomite reservoir. The structural fractures created during the folding of the late Yanshanian-Himalayan orogeny improved the porosity and permeability of the reservoir and, finally, produced an effective fracture-pore type reservoir in the Carboniferous Huanglong Formation in the Eastern Sichuan Basin.

5 Conclusions

1) The dolomites in the Huanglong Formation of Eastern Sichuan Basin can be classified into four genetic categories as follows: (i) the quasi-syngenetic dolomites (Rd1); (ii) early diagenetic burial dolomites (Rd2); (iii) middle diagenetic burial dolomites (Rd3); and (iv) paleo-epidiagenetic dolomites leached and transformed by meteoric water (Bd).

2) The diagenetic fluids responsible for dolomitization of the Huanglong Formation in the Eastern Sichuan Basin can be divided into four types: (i) marine-derived pore waters in the marine diagenetic environment; (ii) sabkha compaction brine preserved in the early shallow-buried diagenetic environment; (iii) strongly-oxidizing low-temperature meteoric water in the seepage-subsurface flow diagenetic environment; and (iv) the strongly reducing deeply seated mixed hot brine in the middle and deep burial diagenetic environment.

3) The fluids developed hereditarily from one environment to another, which resulted in its respective characteristics. Different water-rock reaction mechanisms, products and assemblage features caused different influences on the development of reservoir. (i) dolomitization by marine-derived pore water in the marine diagenetic environment of quasi-syngenetic stage did not form an effective reservoir; (ii) early diagenetic burial dolomitization by the sabkha compaction hot brine was the basis for the development of the reservoirs; (iii) the dissolution of strongly-oxidizing low-temperature meteoric water in the seepage-subsurface flow diagenetic environment of paleo-epidiagenetic stage improved

the reservoir quality; and (iv) deep-burial organic acid dissolution and tectonic fracturing in the reburial diagenetic stage further improved the porosity and permeability of the reservoir, improving the reservoir quality.

References

Amthor J E, Mountjoy E W and Machel H. Subsurface dolomites in Upper Devonian Leduc Formation buildups, central part of Rimbey-Meadowbrook reef trend, Alberta, Canada. Bulletin of Canadian Petroleum Geology. 1993. 41: 164-185

Azmy K, Knight I, Lavoie D, et al. Origin of dolomites in the Boat Harbour Formation, St. George Group, in western Newfoundland, Canada: implications for porosity development. Bulletin of Canadian Petroleum Geology. 2009. 57(1): 81-104

Azomani E, Azmy K, Blamey N, et al. Origin of Lower Ordovician dolomites in eastern Laurentia: Controls on porosity and implications from geochemistry. Marine and Petroleum Geology. 2013. 40: 99-114

Breesch L, Stemmerik L and Wheeler W. Fluid flow reconstruction in a complex paleocave system reservoir in Wordiekammen, Central Spitsbergen. Journal of Geochemical Exploration. 2009. 101(1): 10

Corlett H J and Jones B. Petrographic and geochemical contrasts between calcite- and dolomite-filled burrows in the Middle Devonian Lonely Bay Formation, Northwest Territories, Canada: Implications for dolomite formation in Paleozoic burrows. Journal of Sedimentary Research. 2012. 82(9): 648-663

Derry L A, Keto L S, Jacobsen S B, et al. Sr isotopic variations in Upper Proterozoic carbonates from Svalbard and East Greenland. Geochimica et Cosmochimica Acta. 1989. 53(9): 2331-2339

Frimmel H E. Trace element distribution in Neoproterozoic carbonates as palaeoenvironmental indicator. Chemical Geology. 2009. 258(3-4): 338-353

Gasparrini M, Bechstädt T and Boni M. Massive hydrothermal dolomites in the southwestern Cantabrian Zone (Spain) and their relation to the late Variscan evolution. Marine and Petroleum Geology. 2006. 23(5): 543-568

Geske A, Zorlu J, Richter D K, et al. Impact of diagenesis and low grade metamorphism on isotope ($\delta^{26}Mg$, $\delta^{13}C$, $\delta^{18}O$ and $^{87}Sr/^{86}Sr$) and elemental (Ca, Mg, Mn, Fe and Sr) signatures of Triassic sabkha dolomites. Chemical Geology. 2012. 332-333: 45-64

Götze J, Tichomirowa M, Fuchs H, et al. Geochemistry of agates: a trace element and stable isotope study. Chemical Geology. 2001. 175(3-4): 523-541

Han Y X, li Z, Han D L, et al. The Lower Ordovician matrix dolomite REE characteristics and the reasons in eastern North Tarim Basin. Acta Petrologica Sinica. 2009. 25(10): 2405-2416 (in Chinese)

Hu Z G, Zheng R C, Hu J Z, et al. Geochemical characteristics of rare earth elements of Huanglong Formation dolomites reservoirs in Eastern Sichuan–Northern Chongqing area. Acta Geologica Sinica. 2009. 83(6): 782-790 (in Chinese)

Huang S J, Qing H R, Hu Z W, et al. Closed-system dolomitization and the significance for petroleum and economic geology: An example

from Feixianguan corbonates, Triassic, NE Sichuan Basin of China. Acta Petrologica Sinica. 2007. 23(11): 2955 -2962 (in Chinese)

Huang S J, Qing H R, Huang P P, et al. Evolution of strontium isotopic composition of seawater from Late Permian to Early Triassic based on study of marine carbonates, Zhongliang Mountain, Chongqing, China. Science in China Series D: Earth Sciences. 2008. 51(4): 528-539

Huang S J, Qing H R, Pei C R, et al. Strontium concentration, isotope composition and dolomitization fluids in the Feixianguan Formation of Triassic, Eastern Sichuan of China. Acta Petrologica Sinica. 2006. 22(8): 2123-2132

Keith M L and Weber J N. Carbon and oxygen isotopic composition of selected limestones and fossils. Geochimica et Cosmochimica Acta. 1964. 28(10-11): 1786-1816

Lai X Y, Yu B S, Chen J Y, et al. Thermodynamic conditions of framework grain dissolution of clastic rocks and its application in Kela 2 gas field. Science in China Series D: Earth Sciences. 2005. 48(1): 21-31

Lavoie D and Chi G X. Hydrothermal dolomitization in the Lower Silurian La Vieille Formation in northern New Brunswick: geological context and significance for hydrocarbon exploration. Bulletin of Canadian Petroleum Geology. 2006. 54(4): 380-395

Li Z, Han D L and Shou J F. Diagensis systems and their spatio-temporal attributes in sedimentary basins. Acta Petrologica Sinica. 2006. 22(8): 2151-2164 (in Chinese)

Liu B J. Sedimentary Petrology. Beijing: Geological Publishing House. 1980. 203-210 (in Chinese)

Liu B J. Some problems on the study of sedimentary diagenesis. Acta Sedimentologica Sinica. 2009. 27(5): 787-791 (in Chinese)

Liu C L, Zhao Q H and Wang P X. Correlation between carbon and oxygen isotopic ratios of lacustrine carbonates and types of oil-producing paleolakes. Geochimica. 2001. 30(4): 363-367 (in Chinese)

Liu J Q, Chen W B, Yang P, et al. The Longeni-Angdanrco paelo-oil dolomite geochemical characteristics in southern part of the central uplift zone of Qiangtang Basin and it's significance. Acta Petrologica Sinica. 2008. 24(6): 1379-1389 (in Chinese)

Loucks R G, Mescher P K and McMechan G A. Three dimensional architecture of a coalesced, collapsed-paleocave system in the Lower Ordovician Ellenburger Group, Central Texas. AAPG Bulletin. 2004. 88(5): 545-564

Milliken K L. Diagenesis. In: Middleton G V (ed.). Encyclopedia of Sediments and Sedimentary Rocks. London: Kluwer Academic Publishers. 2003. 214-219

Slater B E and Smith L B. Outcrop analog for Trenton–Black River hydrothermal dolomite reservoirs, Mohawk Valley, New York. AAPG Bulletin. 2012. 96(7): 1369-1388

Smith Jr L B. Origin and reservoir characteristics of upper Ordovician Trenton–Black River hydrothermal dolomite reservoirs in New York. AAPG Bulletin. 2006. 90(11): 1691-1718

Veizer J, Ala D, Azmy K, et al. ^{87}Sr/^{86}Sr, δ^{13}C and δ^{18}O evolution of Phanerozoic seawater. Chemical Geology. 1999. 161(1-3): 58-88

Veizer J. Chemical diagenesis of carbonates: theory and application of trace element technique. In: Stable Isotopes in Sedimentary Geology. 1983

Walter M R, Veevers J J and Calver C R. Dating the 840-544 Ma Neoproterozoic interval by isotopes of strontium, carbon, and sulfur in seawater, and some interpretative models. Precambrian Research. 2000. 100: 371-433

Wang L S, Chen S J, Yang J J, et al. Geochemical characteristics of the Carboniferous reservoir and fluid in Eastern Sichuan Basin, China. Natural Gas Exploration and Development. 2001. 24(3): 28-38 (in Chinese)

Wang S Q, Zhao L, Cheng X B, et al. Geochemical characteristics and genetic model of dolomite reservoirs in the eastern margin of the Pre-Caspian Basin. Petroleum Science. 2012. 9(2): 161-169

Wang X L, Jin Z J, Hu W X, et al. Using in situ REE analysis to study the origin and diagenesis of dolomite of Lower Paleozoic, Tarim Basin. Science in China Series D: Earth Sciences. 2009. 39(6): 721-733

Wang Y G, Wen Y C and Liu Z J. Palaeokarst and burial corrosion in porous evolution of carbonate rock reservoirs of Carboniferous in East Sichuan. Natural Gas Industry. 1996. 16(6): 18-24 (in Chinese)

Wen H G, Zheng R C and Shen Z M. Sedimentary–diagenetic systems of carbonate reservoirs in the Huanglong Formation, Eastern Sichuan Basin. Earth Science—Journal of China University of Geosciences. 2011. 36(1): 111-121 (in Chinese)

Wen H G, Zheng R C, Shen Z M, et al. Study on the Carboniferous palaeokarst landform in Eastern Sichuan Basin. Geological Review. 2009. 55(6): 816-827 (in Chinese)

Zhang B, Zheng R C, Wang X B, et al. Geochemical characteristics and diagenetic systems of dolomite reservoirs of the Changxing Formation in the eastern Sichuan Basin, China. Petroleum Science. 2012. 9(2): 141-153

Zhang X F, Hu W X, Zhang J T, et al. Geochemical analyses on dolomitizing fluids of Lower Ordovician carbonate reservoir in Tarim Basin. Earth Science Frontiers. 2008. 15(2): 80-89 (in Chinese)

Zhao Y F. Genetic mechanism and oil-gas analysis of high and steep structure in East Sichuan. Master's Dissertation. Beijing: China University of Geosciences. 2005. 1-80 (in Chinese)

Zheng R C, Dang L R, Zheng C, et al. Diagenetic system of carbonate reservoir in Huanglong Formation from East Sichuan to North Chongqing area. Acta Petrolei Sinica. 2010. 31(2): 237-245 (in Chinese)

Zheng R C, Hu Z G, Zheng C, et al. Geochemical characteristics of stable isotopes in paleokarst reservoirs in Huanglong Formation in northern Chongqing–eastern Sichuan area. Earth Science Frontiers. 2008. 15(6): 303-311 (in Chinese)

Zheng R C, Liu H N, Wu L, et al. Geochemical characteristics and diagenetic fluid of the Callovian-Oxfordian carbonate reservoirs in Amu Darya Basin. Acta Petrologica Sinica. 2012. 28(3): 961-970 (in Chinese)

Zheng R C, Peng J and Gao H C. Palaeokarst-related characteristics and cycles of carbonate reservoirs in Huanglong Formation, upper Carboniferous, eastern Chongqing. Geology-Geochemistry. 2003. 31(1): 28-35 (in Chinese)

Zheng Y F and Chen J F. Stable Isotope Geochemistry. Beijing: Science Press. 2000. 143-217 (in Chinese)

Zhu D Y, Meng Q Q, Hu W X, et al. Deep Cambrian surface-karst dolomite reservoir and its alteration by later fluid in Tarim Basin. Geological Review. 2012. 58(4): 691-701 (in Chinese)

Zhu R K, Zou C N, Zhang N, et al. Diagenetic fluids evolution and genetic mechanism of tight sandstone gas reservoirs in Upper Triassic Xujiahe Formation in Sichuan Basin, China. Science in China Series D: Earth Sciences. 2009. 51(9): 1340-1353

Appendix 1 Samples, description, elemental and isotopic geochemical compositions in the Huanglong Formation carbonates

Sample id	Phase	Depth m	CaCO₃ %	MgCO₃ %	Sr ppm	Mn ppm	Fe ppm	La ppm	Ce ppm	Nd ppm	Sm ppm	Eu ppm	Tb ppm	Yb ppm	Lu ppm	δ^{13}C, ‰ (VPDB)	δ^{18}O, ‰ (VPDB)	^{87}Sr/^{86}Sr±2σ
BD32	Ml	3945.61			133	75	620									-1.171	-3.301	0.708600±0.000074
BD33	Ml	4023.54			136	69	650									-0.816	-7.106	0.709150±0.000044
LF12	Ml	4702.92			146	81	780	17.21	15.56	14.32	3.56	0.68	0.59	1.24	0.16	-1.73	-8.33	0.709101±0.000032
QB32	Ml	4648.5			150	65	740	18.52	18.32	13.56	3.12	0.71	0.65	1.25	0.19	-1.32	-6.25	0.706972±0.000039
YF12	Ml	5217			180	73	430	15.16	20.44	13.12	3.22	0.61	0.72	1.15	0.12	-1.18	-9.32	0.708972±0.000058
Z4	Ml	3538.43			90	52	420	17.87	22.11	13.77	2.95	0.64	0.47	1.32	0.19	-0.651	-8.928	0.713830±0.000044
Z35	Ml	3529.45			190	53	580	19.74	21.19	14.41	3.15	0.59	0.6	1.03	0.15			
BD13	Rd1	4016.67	53.69	46.31	105	89	810	2.76	4.03	2.82	0.65	0.15	0.18	0.16	0.02	2.31	-2.32	0.713622±0.000056
HX16	Rd1	4591.8	54.33	45.67	374	112	980	1.23	2.23	1.68	0.5	0.1	0.1	0.11	0.01	2.67	-1.23	0.710290±0.000058
J12	Rd1	5714.3			108	100	1400									3.67	-1.22	0.718008±0.000052
QL35	Rd1	4693.2			102	66	830									2.57	-2.1	0.711753±0.000096
T22	Rd1	3380	53.69	46.31	166	135	850	3.08	4.6	3.98	0.75	0.17	0.19	0.19	0.02	2.54	-3.04	0.713990±0.000041
T24	Rd1	3386.3	54.33	45.67	140	105	760	3.18	5.8	4.06	0.87	0.24	0.2	0.18	0.02	2.89	-1.73	0.712877±0.000041
TD25	Rd1	4996.1			134	110	900											
YA18	Rd1	5333.2			87	127	840											
YA28	Rd1	4596.3			120	155	970											
YJ18	Rd1	5268.2			95	92	1600	1.89	2.98	1.76	0.55	0.13	0.12	0.12	0.01	3.95	-1.47	0.709962±0.000111
YJ21	Rd1	5254.2			137	140	860	3.75	6.2	4.38	1.16	0.31	0.23	0.31	0.03	2.42	-1.23	0.709453±0.000043
Z25	Rd1	2920.5	53.69	46.31	93	142	920	0.72	1.41	0.79	0.2	0.06	0.05	0.08	0.01	3.482	-1.869	0.713230±0.000029
Z27	Rd1	3538.43	54.97	45.03	120	125	780	3.75	4.81	4.94	1.14	0.28	0.22	0.41	0.05	2.663	-2.124	0.715704±0.000021
Z31	Rd1	3417.83	54.97	45.03	66	86	830	3.85	6.9	4.58	1.18	0.32	0.25	0.34	0.04	1.774	-1.14	0.711950±0.000091
B2	Rd2	3192.48	52.42	47.58	81	65	1200	0.35	0.3	0.49	0.2	0.06	0.05	0.2	0.03	3.136	-2.171	0.710330±0.000078
BD4	Rd2	4110	54.33	45.67	169	150	1400	8.01	17.42	10.27	2.12	0.57	0.49	1	0.13	0.64	-2.039	0.710800±0.000112
BD6	Rd2	4118.25	53.69	46.31	270	55	1500	4.08	7.93	5.19	1.5	0.39	0.19	0.26	0.03	1.059	-3.061	0.709670±0.000085
BD9	Rd2	4595	51.15	48.85	121	180	1300	11.62	24.9	11.69	2.95	1.07	0.58	2.99	0.42	0.442	-2.64	0.711420±0.000034
C3	Rd2	4385			48	89	1900									1.6	-2.95	0.715152±0.000057
C4	Rd2	4379			76	150	1800									0.93	-5.67	0.714996±0.000032
CZ1	Rd2	5548.86			62	56	2400									3.7	-2.65	0.714038±0.000101
CZ3	Rd2	5559.8			90	145	1500									1.85	-3.69	0.709531±0.000064
DX4	Rd2	4594.3			34	120	1900									2.1	-2.13	0.714503±0.000117
DX7	Rd2	4607.84			60	150	2500									1.49	-3.2	0.710785±0.000040
J8	Rd2	5695.4			63	79	1700											
DX6	Rd2	4603.1			58	110	2300											
HX18	Rd2	4658.35			62	160	1900	1.31	2.24	1.61	0.49	0.15	0.11	0.29	0.04	2.492	-2.846	0.712300±0.000042
J10	Rd2	5705			73	52	2900									3.82	-3.98	0.720409±0.000054
LD7	Rd2	4753.3			80	160	1540									1.64	-4.09	0.709998±0.000067
MC14	Rd2	4119.7			55	240	1200									1.9	-2.97	0.715933±0.000102
MC20	Rd2	4122.8			60	160	1200											
MC21	Rd2	4124.1			45	240	1500									3.84	-2.8	0.715429±0.000122
ML24	Rd2	4492.25			18	300	1800									1.38	-3.94	0.713060±0.000101
ML25	Rd2	4501.12			62	180	1000									2.19	-2.84	0.717072±0.000071

(To be continued)

(Continued)

ML27	Rd2	4508.3			43	140	980									3.12	-3.76	0.716853±0.000025
QL31	Rd2	4707.8			23	210	450									2.32	-3.32	0.713642±0.000081
T21	Rd2	3376	54.33	45.67	48	80	1750	9.43	17.76	11.25	2.88	1.01	0.54	2.06	0.37	2.121	-2.144	0.719040±0.000084
TD26	Rd2	5016.18			39	190	1500									2.79	-3.35	0.715750±0.000045
TD29	Rd2	4459.08			26	170	810									0.2	-4.96	0.716997±0.000051
TD36	Rd2	4595.2			55	84	930									0.91	-2.87	0.707473±0.000059
W13	Rd2	2839.6			62	160	1200									2.69	-2.56	0.712942±0.000059
X24	Rd2	3837.27	54.33	45.67	46	70	1860	0.88	1.01	1.03	0.39	0.09	0.09	0.18	0.02	1.609	-4.145	0.711640±0.000047
YA16	Rd2	5320.6			64	84	1800											
YA29	Rd2	4597.2			86	94	2400											
YA30	Rd2	4622.07			49	170	2000											
YD14	Rd2	5153.1			91	180	2100											
YJ17	Rd2	5271.6			79	98	1600									1.64	-2.83	0.713084±0.000064
Z30	Rd2	3394.39	54.97	45.03	70	230	1500	0.92	1.13	1.29	0.36	0.09	0.09	0.3	0.04	2.579	-2.326	0.711110±0.000065
BD7	Rd2	4118.5			130	130	1950	8.9	13.49	7.1	1.68	0.46	0.25	0.52	0.07	0.704	-3.542	0.712560±0.000029
BD10	Rd3	4600	53.05	46.95	95	220	2800	0.61	1.17	0.78	0.26	0.09	0.02	0.16	0.02	1.056	-6.294	0.710700±0.000090
BD8	Rd3	4578	53.05	46.95	62	195	1700	0.68	1.19	1.22	0.3	0.07	0.03	0.08	0.01	1.32	-5.32	0.714211±0.000027
CZ4	Rd3	5558.5			69	226	1900									1.45	-6.12	0.714941±0.000025
HX17	Rd3	4650.01	53.05	46.95	117	260	2450	2.21	2.38	1.92	0.69	0.22	0.06	0.49	0.07	0.45	-8.891	0.709220±0.000039
LB19	Rd3	3044.28	53.05	46.95	78	180	2100	2.45	3.63	3.18	0.94	0.6	0.09	0.5	0.08	0.766	-6.097	0.713820±0.000059
LB20	Rd3	3886.12	53.69	46.31	85	220	2500	2.23	3.02	1.93	0.41	0.1	0.04	0.29	0.04	2.048	-4.125	0.711840±0.000045
LD8	Rd3	4710			74	460	2100									1.07	-5.07	0.714321±0.000031
MC13	Rd3	4176.3			61	190	2500									1.64	-5.37	0.713455±0.000090
TD21	Rd3	4920.61			42	170	1100									2.6	-3.84	0.711934±0.000037
TD23	Rd3	4918.2			40	180	2400									1.68	-4.74	0.714945±0.000081
TD28	Rd3	4982.89			28	300	1800									0.36	-3.31	0.712118±0.000041
Z29	Rd3	3887.83	53.69	46.31	130	260	1900	1.61	1.81	0.85	0.33	0.11	0.04	0.08	0.01	1.305	-6.055	0.712710±0.000040
Z28	Rd3	3542.84	54.97	45.03	103	280	3200	2.3	2.7	1.39	0.58	0.19	0.04	0.4	0.05	3.339	-3.125	0.712250±0.000097
B3	Bd	3225.11			25	180	3600	0.97	1.64	0.98	0.35	0.07	0.08	0.11	0.01	2.208	-4.028	0.712540±0.000092
B4	Bd	2415.79			22	130	4200	1.04	1.86	1.22	0.41	0.09	0.11	0.15	0.02	2.613	-5.525	0.710651±0.000078
HX15	Bd	4580.33			30	150	3500	1.11	2.17	1.45	0.57	0.11	0.14	0.29	0.04	2.278	-2.536	0.712271±0.000022
MC17	Bd	4123.2			54	210	3300									2.24	-4.76	0.715111±0.000071
MC18	Bd	4123.2			27	280	6100									2.12	-4.34	0.715751±0.000046
MC22	Bd	4123.86			30	320	5600									1.14	-3.93	0.712338±0.000031
QL32	Bd	4696.3			71	140	820									1.62	-2.44	0.718115±0.000080
QL33	Bd	4696.3			43	150	1200									1.6	-4.39	0.719975±0.000045
QL39	Bd	3001.5			15	240	4600									2.61	-4.43	0.719166±0.000053
QL38	Bd	3001.5			65	139	2750									0.64	-4.2	0.717653±0.000043
QL45	Bd	2974.3			35	232	3300									0.33	-4.05	0.719142±0.000042
TD30	Bd	4915.2			55	160	4300									2.52	-4.11	0.714396±0.000046
TD31	Bd	4915.2			20	220	4800									2.41	-4.36	0.714974±0.000073
YA26	Bd	4617.2			20	192	5200	0.99	1.68	1.32	0.47	0.09	0.12	0.14	0.02	1.21	-3.65	0.718980±0.000025
Z26	Bd	2927			23	120	3600	1.04	1.61	0.98	0.41	0.08	0.09	0.16	0.02	3.942	-3.369	0.711870±0.000074
Z36	Bd	3540			26	260	3200	1.58	1.84	1.46	0.5	0.1	0.12	0.27	0.03	1.249	-4.405	0.706510±0.000014